Published online 27 January 2012 *Nucleic Acids Research, 2012, Vol. 40, No. 10* ***4347–4357***
doi:10.1093/nar/gks029

Regulation of Enteric *vapBC* Transcription: Induction by VapC Toxin Dimer-Breaking

Kristoffer S. Winther and Kenn Gerdes*

Centre for Bacterial Cell Biology, Institute for Cell and Molecular Biosciences, Newcastle University, NE2 4AX Newcastle, UK

Received November 3, 2011; Revised January 3, 2012; Accepted January 5, 2012

ABSTRACT

Toxin-antitoxin (TA) loci encode inhibitors of translation, replication or cell wall synthesis and are common elements of prokaryotic plasmids and chromosomes. Ten TA loci of *Escherichia coli* K-12 encode mRNases that cumulatively contribute to persistence (multidrug tolerance) of the bacterial cells. The mechanisms underlying induction and reversion of the persistent state are not yet understood. The *vapBC* operon of *Salmonalla enterica* serovar Typhimurium LT2 encodes VapC, a tRNase that reversibly inhibits translation by site-specific cleavage of $tRNA^{fMet}$. VapB is an antitoxin that interacts with and neutralizes VapC via its C-terminal tail and regulate TA operon transcription via its N-terminal DNA binding domain that recognize operators in the *vapBC* promoter region. We show here that transcription of the *vapBC* operon of *S. enterica* is controlled by a recently discovered regulatory theme referred to as 'conditional cooperativity': at low T/A ratios, the TA complex binds cooperatively to the promoter region and represses TA operon transcription whereas at high T/A ratios, the excess toxin leads to destabilization of the TA-operator complex and therefore, induction of transcription. We present evidence that an excess of VapC toxin leads to operator complex destabilization by breaking of toxin dimers.

INTRODUCTION

Prokaryotic chromosomes and plasmids encode a plethora of toxin–antitoxin (TA) loci that belong to three different types. In type I TA loci, the antitoxin is a *cis*-encoded antisense RNA that inhibits translation of a toxin-encoding mRNA (1,2). In type II loci, the antitoxin is a protein that combines with and neutralizes the cognate toxin (3). Finally, in type III loci, the antitoxin is an RNA that combines with and neutralizes the toxin (4). Type II TA loci are common and, based on toxin sequence similarities, have been divided into evolutionary independent gene families (5,6). Three of these families, *vapBC*, *relBE* and *hicAB* are common in both bacteria and archaea (5,7,8). Of these three families, *vapBC* loci are particularly abundant: of approximately 3825 TA loci identified in 900 prokaryotic genomes, approximately 1300 were *vapBC* loci (9). In some organisms, the numbers of TA loci are particularly high. Remarkably, *Mycobacterium tuberculosis* has at least 88 type II TA loci, 45 of which are *vapBC* homologues (10). The reason for the large expansions of TA loci in particular organisms is not known.

TA loci have been linked to several biological functions, such as plasmid and gene stabilization (11,12) and environmental stresses, such as amino acid starvation (13). It has also been suggested that TA loci have no biological function (14). However, recently we showed that, in the model organism *Escherichia coli*, TA loci were required for bacterial persistence (15). Thus, progressive deletion of type II TA loci gradually reduced the persistence level and deletion of 10 TA loci encoding RNA endonucleases reduced persistence approximately 200-fold.

Even though the different families of type II TA loci have independent evolutionary origins their regulation and genetic organization are remarkably similar. In almost all cases, a TA locus consists of two closely linked genes, one of which encodes the antitoxin and the other the toxin. Although rare exceptions exists (16,17), transcription of almost all type II TA operons is autoregulated by the TA complex that binds to one or more operators in the TA promoter region. The TA complex binds to DNA via a domains present in the antitoxin. Usually, the toxin enhances the binding of the antitoxin to the operator (3). The DNA domains belong to four different classes: Helix–Turn–Helix (HTH), Ribbon–Helix–Helix (RHH), AbrB and Phd/YefM (3). In the *vapBC* and *relBE* gene

*To whom correspondence should be addressed. Tel: +44 191 208 3230; Fax: +44 191 208 3205; Email: Kenn.Gerdes@newcastle.ac.uk

families, the antitoxins can have any of these four DNA binding motifs, indicating that domain shuffling took place during the evolution of these gene families (6).

In actively growing cells, the TA operators are occupied by cognate TA complexes and transcription of the operons is repressed (13,18–22). The antitoxins are metabolically unstable due to degradation by cellular proteases. For example, Lon degrades RelB antitoxin of *E. coli* (13). In growing cells, *de novo* synthesis of RelB replenishes the RelB pool and *relBE* translation stays repressed. In contrast, when translation is reduced by, e.g. amino acid starvation, the RelB level is reduced. Consequently, the TA promoter is activated (13). In turn, the increased transcription-rate of *relBE* leads to partial replenishment of the antitoxin pool after an initial delay (13,23). Even though the antitoxin level is restored to 50% of the initial pre-starvation level, the transcription-rate of the TA operon stays unexpectedly high during amino acid starvation (13). More in-depth analysis revealed that transcription of *relBE* is regulated by the RelB/RelE ratio such that when [RelB] > [RelE], two $RelB_2$•RelE complexes bind strongly and cooperatively to two operators (*relO*) overlapping the *relBE* promoter sequences and repress transcription (23). In contrast, when [RelB] < [RelE], the excess RelE invades the $RelB_2$•RelE•*relO* complex and abolishes cooperative binding, probably via the formation of a $RelB_2$•$RelE_2$ tetramer that does not bind cooperatively to *relO*. By this mechanism that we called 'conditional cooperativity', the RelB/RelE ratio controls the transcription-rate of *relBE* (23). In turn, the RelB/RelE ratio is controlled by the interplay of the *relBE* translation-rate and the degradation-rate of RelB that is determined by Lon. Transcription of the *phd doc* and *ccd* operons of plasmid P1 and F is also regulated by conditional cooperativity (24,36). That evolutionarily unrelated TA loci are regulated by conditional cooperativity by different molecular mechanisms indicates that this peculiar mode of transcriptional regulation is a biologically important property of TA loci.

Here we investigate if conditional cooperativity controls transcription of an enteric *vapBC* locus. VapC toxins from enterobacteria are tRNases that inhibit global translation by site-specific cleavage of $tRNA^{fMet}$ between the anticodon stem and loop (25). As with other TA loci, VapBC complexes bind to operators in the promoter regions and autoregulate transcription (26–28). Structural analysis of VapBC from *Neisseria gonorrhoeae* (also called FitAB) showed that an octamer of four VapB–VapC heterodimers $[(VapBC)_2]_2$ binds to operator DNA via an RHH motif in VapB (29), consistent with autoregulation of *vapBC* transcription by VapBC.

We show that VapB of *Salmonella enterica* serovar Typhimurium LT2 that contains an AbrB-like DNA-binding motif is degraded by the ATP-dependent Lon protease. When translation is inhibited, VapB decays and *vapBC* promoter activity increases, consistent with transcriptional autoregulation by VapB. Indeed, VapB binds to two operator sequences (*vapO1* and *vapO2*) in the promoter region *in vitro* and this binding is strongly enhanced by VapC. Remarkably, an excess of VapC decreases the affinity of the VapBC complex for DNA and, consistently, increases transcription-rate *in vivo*. Structural modelling and mutational analysis allow us to propose a novel mechanism of conditional cooperativity in which excess VapC toxin induces *vapBC* transcription by breaking of VapC dimers.

MATERIALS AND METHODS

Media, antibiotics, strains and plasmids

Bacteria were grown in Luria–Bertani medium (LB) as described (30). When required, the medium was supplemented with 30 or 100 μg/ml ampicillin, 50 μg/ml chloramphenicol, 25 μg/ml kanamycin. X-gal (5-bromo-4-chloro-3-indoyl-b-D-galactoside) was added to a final concentration of 40 μg/ml. Expression of proteins from the $P_{A1/O4/O3}$ or P_{BAD} promoters was induced by 2 mM isopropylb-D-thiogalactopyranoside (IPTG) or 0.2% arabinose, respectively. Strains and plasmids are listed in Supplementary Table S1 and oligonucleotides in Supplementary Table S2, respectively.

Purification of VapB and VapC proteins

VapC and VapB were purified essentially according to (25). Strain C41 containing pKW512HB, pKW512HB L43A, pKW512HBI44A, pKW512HBY72A, pKW512 HBA76S or pKW512HC was grown exponentially under aeration in LB at 37°C. At OD_{450} = 0.5, expression was induced by addition of 2 mM IPTG. After 3 h of growth, the culture was harvested and resuspended in ice-cold lysis buffer (50 mM NaH_2PO_4, 0.3 M NaCl, 10 mM imidazole, 5 mM β-mercaptoethanol pH8 supplemented with EDTA-free protease inhibitor, Roche). Cells were disrupted using a Constant Cell disruption system and lysate cleared by centrifugation at 15 000 rpm for 30 min at 4°C. The cleared lysate was then incubated with Ni-NTA agarose (Qiagen) for at least 2 h at 4°C and subsequently loaded onto a gravity column. The column was washed extensively in wash buffer (50 mM NaH_2PO_4, 0.3 M NaCl, 35 mM imidazole, 5 mM β-mercaptoethanol pH 8). VapC or VapB was then eluted from complex under denaturing conditions by incubating the column overnight (ON) at room-temperature in 10 column volumes of denaturing buffer (100 mM NaH_2PO_4, 10 mM Tris–HCl, 9.8 M Urea, pH8). Denatured protein was refolded by four-step dialysis; (i) 1 × PBS 0.1% Triton X-100 5 mM DTT, (ii) 1 × PBS 5 mM DTT, (iii) 1 × PBS 5 mM DTT and (iv) 1× PBS 20% glycerol 1 mM DTT. The authenticity and purity was verified by SDS–PAGE.

Electrophoretic mobility shift assays and DNase I footprinting

DNA fragments were constructed containing either one binding site *vapO1* (using hybridized oligos VapBC binding#small-down and VapBCbinding#small-up) or two binding sites, *vapO1 and vapO2* (PCR product with oligos vapBC_EMSA_down and vapBC_EMSA_up). Prior to the hybridization and PCR reaction VapBC binding#small-down or vapBC_EMSA_down were

5′-end-labelled with [γ-32P]ATP using T4 polynucleotide Kinase (New England Biolabs). Binding site mutations in *vapO1* and *vapO2* were introduced by PCR using primers PBC-10_MUT_DOWN and PBC-10_MUT_UP for site 1 and PBC-35_MUT_DOWN and PBC-35_MUT_UP for site 2. Labelled probes (0.5–2 nM) were incubated with purified proteins in binding buffer (20 mM Tris–HCl pH 7.5, 100 mM KCl, 2 mM $MgCl_2$, 1 mM DTT, 50 μg/ml BSA and 10% glycerol) to avoid unspecific DNA binding sonicated salmon sperm DNA (ssDNA) was added to a final concentration 0.1 mg/ml. Reactions were incubated for 20 min at 37°C before DNA bound complexes were separated by native PAGE in 5% or 6% acrylamide gels with 0.5× TBE for two and one binding site probes, respectively. The separation was followed by phosphorimaging.

For DNase I footprinting, samples were incubated with 0.01 U/μl DNase I and 1 × DNase I buffer (Roche) at 37°C for 2 min, followed by addition of 100 μl of Stop buffer (2 M ammonium acetate, 20 mM EDTA, 10 mg/ml ssDNA). The resulting DNA fragments were extracted once in phenol, once in chloroform, precipitated in ethanol and separated on an 8% denaturing acrylamide gel along with a dideoxyNTP sequencing ladder. The digestion pattern was analysed by to phosphorimaging.

RESULTS

VapB autoregulates *vapBC* transcription and is degraded by Lon protease

VapB of *S. enterica* LT2 (STM3034) contains an AbrB DNA binding domain in its N-terminus (31), raising the possibility that VapB autoregulates *vapBC* transcription via binding to two inverted repeats in the promoter region that we call *vapO1* and *vapO2* (Figure 1A). The entire operator was called *vapO*. Previously, we showed that amino acid starvation induces *vapBC* transcription (32). We examined *vapBC* transcription using primer extension analysis of RNA prepared from strains *S. enterica* LT2 (KP1001) or *E. coli* K-12 (MG1655, *wt*) carrying *vapBC* on a low-copy-number plasmid before and after the inhibition of translation by the addition of chloramphenicol. As seen from Figure 1B, the level of transcripts increased in both strains. Transcription also increased in strain MG1655Δ*clpP* but not in the isogenic Δ*lon* strain, suggesting that Lon protease degrades VapB. To test this inference directly, we measured VapB levels. As seen from Figure 1C, VapB decayed rapidly in *wt* and Δ*clp* but not in the Δ*lon* strain. Thus, Lon degrades VapB. The increased mRNA level seen after inhibition of translation with chloramphenicol suggested that VapB autoregulates

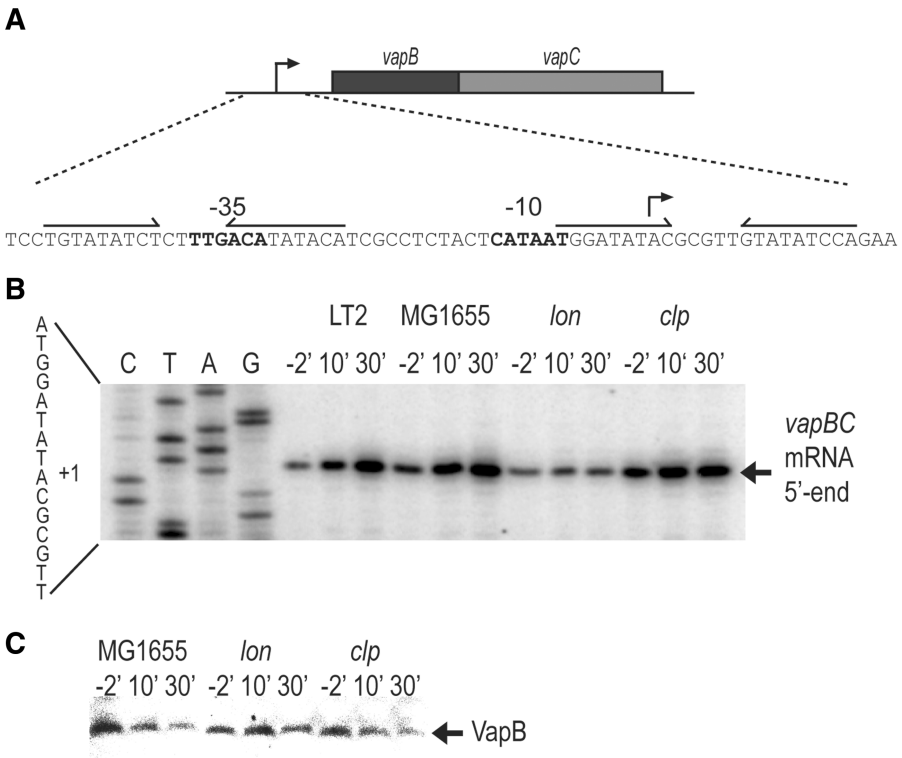

Figure 1. Lon degrades VapB and is required for activation of *vapBC* transcription. (**A**) DNA sequence of the *vapBC* promoter region showing −10 and −35 promoter sequences and the two operators *vapO1* and *vapO2* as inverted repeats. (**B**) Primer extension analysis of the 5′-end of *vapBC* mRNA. Strains MG1655 (*E. coli* K-12, *wt*), KW10 (MG1655*Δlon*) or KW11 (MG1655*ΔclpP*) containing pKW71512 (pNDM71*::vapBC*) and KP1001 (*S. enterica* LT2) were grown exponentially in LB medium. At time zero, chloramphenicol (50 μg/ml) was added and cell samples were withdrawn at the time points indicated (min). Total RNA was extracted and reverse transcription was performed using primer vapB-5#PE. (**C**) Western blotting analysis of VapB. MG1655 KW10 or KW11 containing pKW51 (pA1/03/04::SD_{opt}*::vapB*) were grown exponentially in LB medium. Ten minutes before the addition of chloramphenicol (50 μg/ml; $t' = 0$), 1 mM IPTG was added to induce *vapB*. Samples were taken at the time points indicated and VapB detected by polyclonal antibodies directed towards VapB.

vapBC transcription, possibly via binding to *vapO1* and *vapO2* that overlap with the −10 and −35 promoter sequences, respectively (Figure 1A).

VapC enhances binding of VapB to *vapO1* and *vapO2*

Native VapB and VapC were purified and used in gel shift analysis to probe their binding to *vapO*. VapB alone formed a complex with *vapO*-encoding DNA (C1 and C2 in Figure 2A); however only at very high concentrations more significant DNA–VapB complexes were observed (lanes 3–7). In contrast, VapB did not bind to a control DNA fragment (P in Figure 2A). Thus, VapB has low but specific affinity for *vapO*. In contrast, VapC alone bound neither to the *vapO* fragment (U) nor to the control fragment (lane 8). However, addition of VapC to a low concentration of VapB yielded an increase in complex formation that further increased dramatically with increasing concentration of VapC (lanes 9–13). Thus, VapC enhances the binding of VapB to *vapO*. Interestingly, at very high concentrations, VapB alone produced a complex with a mobility similar to that generated by VapBC (Figure 2A, comp. lanes 3–7 with lanes 9–14). This could be due to the presence of a small amount of VapC in the VapB preparation or because the complexes were complexes are not resolved in this experimental setup.

Next, we performed foot printing analysis of the complex bound to *vapO*. DNA was incubated with a constant concentration of VapB and increasing concentrations of VapC and digested with DNase I (Figure 2B, lanes 1–4). Two protected regions overlapping with the two inverted repeats appeared, consistent with VapBC binding to *vapO1* and *vapO2*. This observation raised the possibility that complexes C1 and C2 observed in the gel shift analysis (Figure 2A) corresponded to one and two VapBC complexes bound to *vapO*, respectively. Most importantly, increasing the concentration of VapC increased VapB binding to operator DNA.

An excess of VapC releases VapBC from operator DNA

At a VapB/VapC ratio of ~2/16 in the gel shift analysis shown in Figure 2A, the amount of C2 complex decreased modestly in intensity while that of C1 increased (lane 14), thus raising the possibility that very high concentrations of VapC destabilized the VapBC*O* complex. To investigate this phenomenon further, we performed gel shift and foot printing analysis with higher concentrations of VapC. As before, increasing [VapC] increased VapB specific binding to *vapO* (Figure 3A, lanes 2 and 3). However, increasing [VapC] further severely reduced binding (lanes 4–8) with almost no VapBC bound at a B/C ratio of 1/16 (lane 8). To investigate if the destabilization of VapBC binding to *vapO* was reversible, we then increased the VapB/VapC ratio by increasing [VapB] while keeping [VapC] constant (lanes 9–11). We observed a resulting increase in binding to *vapO*, consistent with a reversible and direct effect of VapC.

DNase I foot printing yielded more detailed information. First, at high [VapC], *vapO1* and *vapO2* were both protected (Figure 3B, lane 2); however, *vapO1* was clearly protected better than *vapO2* and an increase of [VapC] released VapBC binding at *vapO2* before *vapO1* (lanes 2–7). When the VapB/VapC ratio was increased, protection was regained (lanes 8 and 9). Again, *vapO1* was protected at a lower concentration of VapB (lane 8) than *vapO2* (lane 9), consistent with higher affinity of the VapBC complex for *vapO1*.

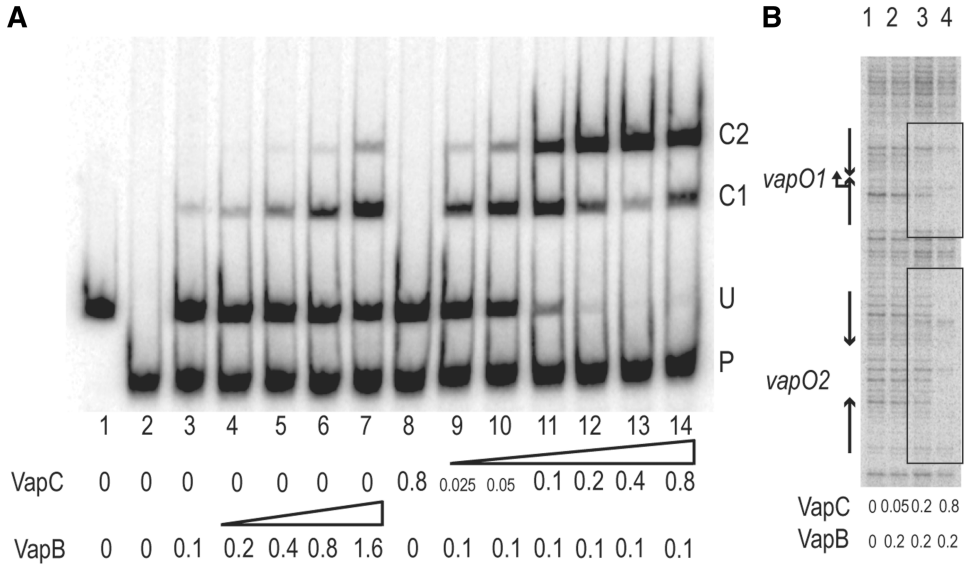

Figure 2. VapC increases the affinity of VapB for *vapO*-encoding DNA. (**A**) VapB and VapBC complex binding to *vapO* analysed by gel shifting. Purified VapB and VapC were added to a 302-bp ^{32}P-labelled *vapO* DNA probe (labelled U in the gel) and a 199-bp mock DNA fragment derived from pUC19 (labelled P). Concentrations of VapB and VapC are given below each lane (μM). C1 and C2 denote the inferred VapBC•*vapO* complexeses. (**B**) VapBC binding to a *vapO*-encoding DNA fragment analysed by DNase I protection. Purified VapB and VapC were added to the same DNA probe as in (A) and subsequently incubated with DNase I (lanes 1–4). The protected regions are enclosed by boxes and the positions of the transcriptional start site and the two inverted repeats are marked with arrows.

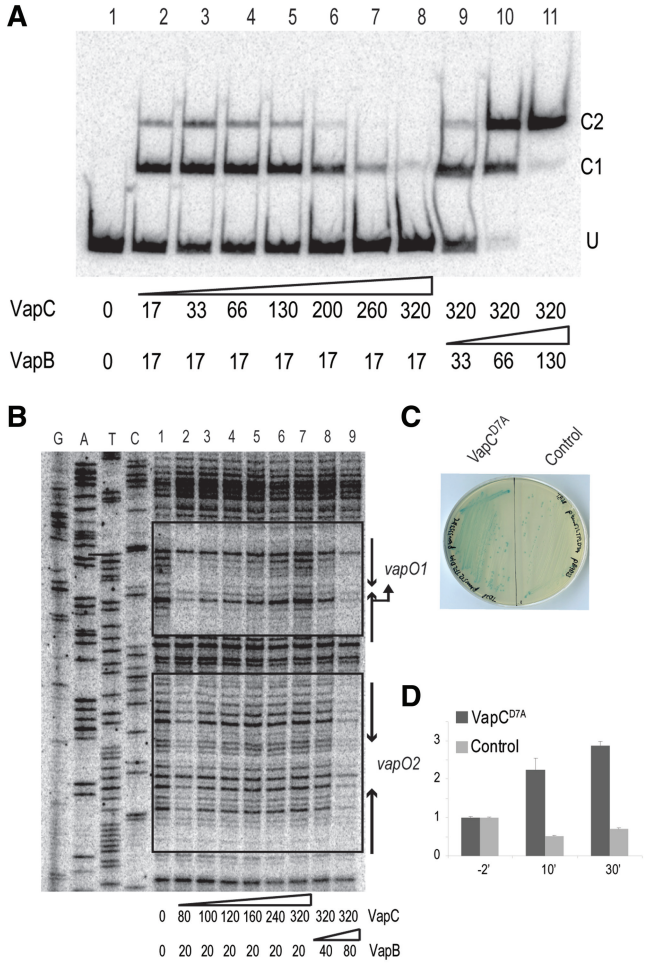

Figure 3. The *vapBC* promoter is controlled by conditional cooperativity. (**A**) Binding of VapB and VapBC complex to a *vapO*-encoding DNA fragment analysed by gel shifting. Purified VapB and VapC were added to a 302-bp ^{32}P-labelled *vapO* probe (lanes 1–11; numbers below the gel are in nM). Protein–DNA complexes were separated by 5% native PAGE. U denotes unbound *vapO* DNA and C1 and C2 VapBC*O* complexes. (**B**) DNase I protection assay of *vapO*. VapB and VapC were incubated with *vapO* DNA as in (A) and subsequently incubated with DNase I (lanes 1–9; numbers are pmol). A DNA sequencing ladder was generated using 5′-end labelled vapBC_EMSA_down primer. Inverted repeats sites 1 and 2 and promoter sequences are indicated by arrows. DNAse I protected bases are enclosed by boxes. (**C**) Ectopic expression of VapC^{D7A} *in vivo* induces *vapBC* transcription. TB28 (MG1655*ΔlacIZYA*) pKW512TFZD7A (*vapBC*^{D7A}::*lacZYA*) containing either pKW3353HC (pBAD::SD$_{opt}$::*vapC*^{D7A}) or pBAD33 were streaked to single colonies on LB plates containing X-gal and 0.2% arabinose. (**D**) VapC^{D7A} induced transcription quantified by qPCR. TB28 (MG1655 *ΔlacIZYA*) pKW512TFZD7A (*vapBC*^{D7A}::*lacZYA*) with pKW3353HC (pBAD::SD$_{opt}$::*vapC*^{D7A}-H6) or pBAD33 (empty vector plasmid) were grown exponentially in LB medium. At 0′, arabinose was added to induce transcription from the pBAD promoter. Samples were taken at time points indicated (min) and total RNA extracted. Fold-of-changes relative to house keeping gene *rpsA* mRNA were measured by quantitative RT-PCR.

An excess of VapC stimulates *vapBC* transcription

The above-described results showed that excess VapC destabilized the VapBC*O* complex and predicted that an excess of VapC in living cells would derepress the *vapBC* promoter. To test this, we fused *vapBC* transcriptionally to the *lacZ* gene. Induction *in trans* of *vapC*^{D7A}, encoding a non-toxic VapC^{D7A} variant, increased LacZ expression from the *vapBC::lacZ* transcriptional fusion (Figure 3C). Induction of *vapBC* by excess VapC^{D7A} was confirmed by quantitative RT-PCR measurements (Figure 3D). After 30′ of induction of *vapC*^{D7A}, the transcription rate of *vapBC::lacZ* had increased ~3-fold. No increase was observed with the control plasmid. This result was consistent with the VapC-mediated destabilization of the VapBC*O* complex seen *in vitro*. Thus, *vapBC* operon transcription is regulated by conditional cooperativity *in vivo*.

One operator site is sufficient for regulation by conditional cooperativity

The definition of conditional cooperativity in TA locus regulation entails cooperative binding of the TA complex to the promoter when the antitoxin is in excess and release of the complex when the toxin is in excess (23,24). To investigate the function of *vapO1* and *vapO2* in the cooperative binding of VapBC to *vapO*, we introduced mutations in the half-sites of *vapO1* and *vapO2*, respectively (Figure 4A). To avoid interference with promoter activity, the mutations were located away from the −10 and −35 promoter sequences (see below). First, we analysed *vapO1*^{Mut} and *vapO2*^{Mut} in gel shift assays (Figure 4B). As before, a *vapO*^{wt} fragment generated two complexes (C1 and C2) that decreased in intensity with increasing concentration of VapC. The *vapO1*^{Mut} and *vapO2*^{Mut} fragments exhibited changed patterns: the C2 complex disappeared (*vapO2*^{Mut}) or was highly reduced (*vapO1*^{Mut}). This pattern supported that the C1 and C2 complexes corresponded to *vapO* bound with one and two VapBC complexes, respectively. Most importantly, however, complex formation was in both cases again reduced when VapC was increased. This result suggested that a single *vapO* operator was sufficient for transcriptional regulation by conditional cooperativity. The fact that C1 complexes formed by *vapO1*^{Mut} and *vapO2*^{Mut} migrate so similarly suggests that the VapBC protein complexes formed on either *vapO1* or *vapO2* are identical. A fragment carrying the double *vapO12*^{Mut} mutation hardly bound VapBC at all, although a faint C1 complex was observed that most likely reflected incomplete disruption of VapBC bound to the *vapO1*^{Mut}. This inference is also consistent with the weak C2 complex seen with the *vapO1*^{Mut} fragment. Nevertheless, the *vapO1* mutation decreased the amount of complex formation more than the *vapO2* mutation, consistent with the observation that the VapBC complex has the highest affinity for *vapO1*.

To investigate the effect of the *vapO* mutations (Figure 4A) on transcriptional repression *in vivo*, we again used transcriptional *vapBC-lacZ* fusions (Figure 4C). The double *vapO1*^{Mut} and *vapO2*^{Mut} mutant (*vapO12*^{Mut}) caused a strong derepression of *vapBC* transcription, consistent with the lack of VapBC binding to the operator sites seen *in vitro*. The single *vapO* mutations also derepressed *vapBC* transcription, but to a much lesser

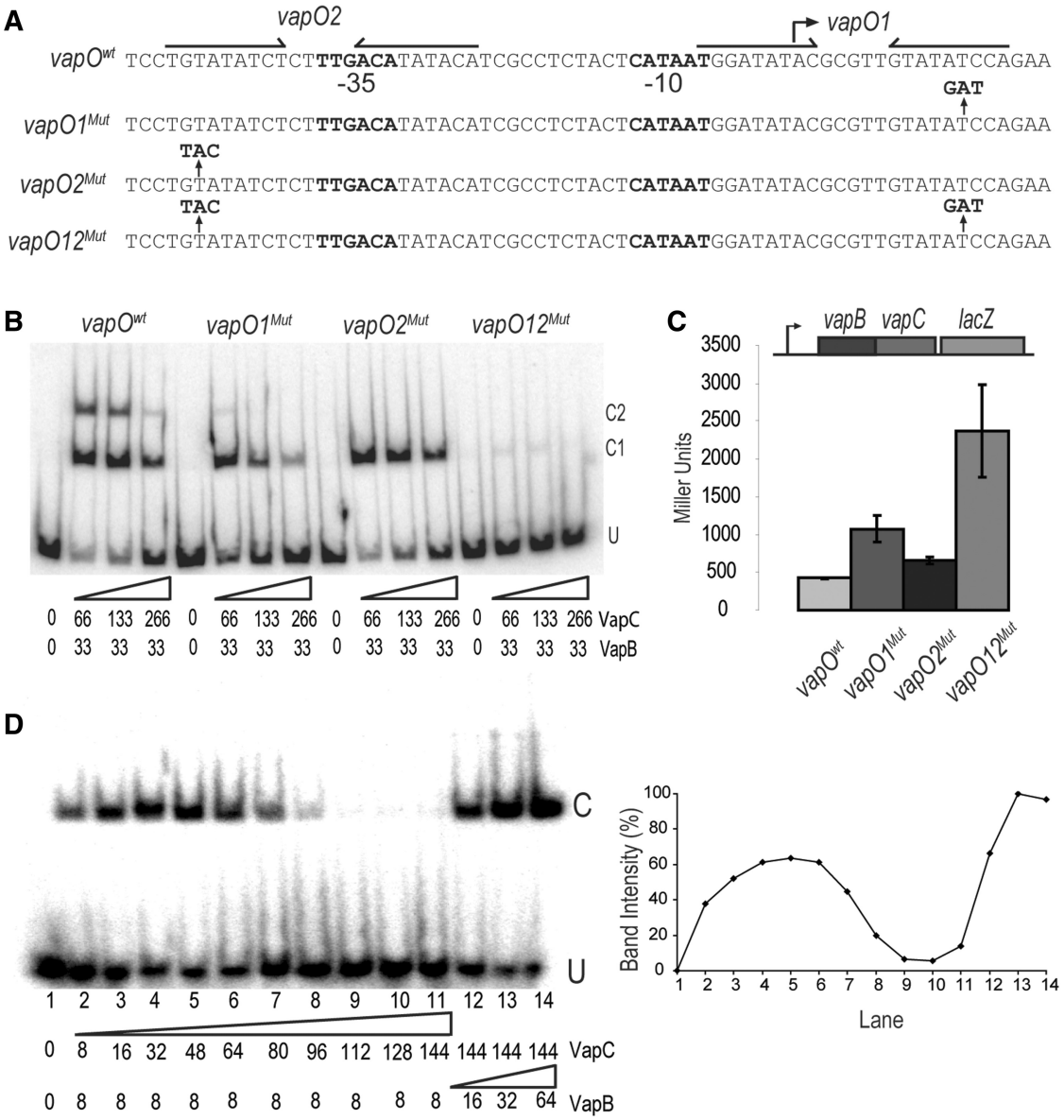

Figure 4. One *vapBC* operator is sufficient for regulation by conditional cooperativity. (**A**) DNA sequences of the *vapBC* promoter region showing the base substitutions in $vapO1^{Mut}$, $vapO2^{Mut}$ and $vapO12^{Mut}$. Inverted repeats are indicated by arrows and promoter sequences by −10 and −35, respectively. (**B**) Gel shift assay of VapBC complex binding to the DNA fragments shown in (A). VapB and VapC were incubated with DNA (numbers are in nM) . U indicates unbound DNA fragment, C1 and C2 are fragments bound by either one or two VapBC complexes, respectively. (**C**) *vapBC* promoter activity in binding site mutants. TB28 (MG1655*ΔlacIZYA*) containing either P*wt*::$vapBC^{D7A}$::*lacZYA* (pKW512TFZD7A), P::$vapO1^{Mut}$::$vapBC^{D7A}$::*lacZYA* (pKW512TFZD7A-1), P::$vapO2^{Mut}$::$vapBC^{D7A}$::*lacZYA* (pKW512TFZD7A-2) or P::$vapO1^{Mut}$::$vapO2^{Mut}$::$vapBC^{D7A}$::*lacZYA* (pKW512TFZD7A-1-2) were grown exponentially in LB medium at 37°C. At an OD_{600} of approximately 0.5, samples were collected and LacZ activity measured (Miller Units). (**D**) Gel shift analysis as in (B) but with a promoter DNA fragment (36 bp) containing only *vapO1*. Numbers below the gel are protein concentrations in nM (lane 1–14). Protein–DNA complexes were separated by 6% native PAGE. U and C indicate positions of unbound and bound DNA, respectively. Insert at right: Quantification of the C band-intensities (%) in the gel-shift shown at left.

extent. The $vapO1^{Mut}$ yielded stronger derepression than $vapO2^{Mut}$, consistent with higher affinity of VapBC for *vapO1* (Figure 4B). Importantly, these observations showed that *vapO1* and *vapO2* can function independently to regulate *vapBC* transcription.

The above-described results raised the possibility that a fragment containing one VapBC binding site would respond with conditional cooperativity at increased VapC/VapB ratios. To test this, we performed gel shift assays using a DNA fragment containing only *vapO1* (Figure 4D). As before, increasing [VapC] increased VapB binding (lanes 2–5). As before, at increased VapC/VapB ratios (2/16, lane 6), binding was reduced and finally totally abolished (lanes 9–11). In these reactions, binding could also be regained by increasing the concentration of VapB (lanes 12–14). Quantification showed the dramatic changes in VapBC binding as a function of the VapC/VapB ratio (Figure 4D).

Mutations in the VapC dimer interface derepress *vapBC* transcription

The crystal structure of a VapBC homologous complex of *N. gonorrhoea* (FitAB, fast intracellular trafficking) revealed an octamer of four VapBC heterodimers $[(VapBC)_2]_2$ bound to operator DNA (Supplementary Figure S1D) (29). In this structure, VapC form bridges between two VapB dimers bound to operator half-sites. The structure readily explains why VapC mediates strong cooperative binding of VapB to operator DNA (29). More recently, the crystal structure of the VapBC complex from *Shigella flexneri* 2a YSH6000 virulence plasmid pMYSH6000 ($VapBC_{S.flex}$) was solved, revealing a similar but more compact structure (Supplementary Figure S1C) (33). This observation implies that VapBC complexes in general form octameric complexes. For the *S. enterica* proteins, the theoretical molecular weight of a $[(VapBC)_2]_2$ octamer is 93.2 kD. Our estimation of the size of the VapBC complex bound to *vapO1* was 92 ± 10 kD (Supplementary Figure S2A–S2D). We infer that VapBC of *S. enterica* also binds as an octameric $[(VapBC)_2]_2$ complex to operator DNA. A similar complex is very likely also formed at *vapO2*.

The FitAB crystal structure (Supplementary Figure S1C and S1D) predicts that VapC dimerization is essential for cooperative binding of the $[(VapBC)_2]_2$ complex to *vapO*. Therefore, the VapC mediated destabilization of the $[(VapBC)_2]_2$•*vapO1* complex can be explained by breaking of the VapC dimer by an excess of VapC (see Discussion). We modelled the tertiary structure of VapC using Phyre (34) and aligned the predicted structure with $VapC_{S.flex}$ and FitB (Supplementary Figure S1B). The primary sequences of VapC and FitB exhibit low similarity (22% identical, 41% similar, Supplementary Figure S1A). However, a VapC dimer aligned well with the FitB dimer in the tetrameric $[(FitAB)_2]_2$•DNA complex and with the $VapC_{S.flex}$ dimer in *S. flexneri* $[(VapBC)_2]_2$ complex (Supplementary Figure S1C and S1D). The modelled structure of the VapC dimer is shown in Figure 5A. This model predicted two patches in VapC to be involved in dimerization. The effect of changing these residues to alanine (or to serine in one case) on *vapBC* transcription was measured using a *vapBC::lacZ* transcriptional fusion (Figure 5B). Changing four residues L43A, I44A, Y72A and A76S individually significantly increased *vapBC* transcription (5.2-, 1.4-, 7.0- and 1.9-fold, respectively). The activity of the $vapBC^{Y72A}$*::lacZ* fusion was similar to that of a *vapBC::lacZ* fusion carrying mutations in both operator sites (comp. Figures 4B and 5C), indicating that the Y72A substitution in VapC resulted in complete loss of repression by the VapBC complex. The tertiary structure alignments showed that tyrosine 72 of VapC and $VapC_{S.flex}$ corresponds to phenylalanine 78 in FitB, a key residue for FitB dimerization (Supplementary Figure S1B) (29). These results support that VapC dimerization is important for repression of *vapBC* transcription by the VapBC complex.

To challenge this inference directly, we asked if the Y72A mutation would affect VapC dimerization. As seen from Supplementary Figure S3, indeed the Y72A mutation abolished dimerization of purified VapC. Thus, we conclude that dimerization of VapC is required for repression of the *vapBC* promoter by the VapBC complex.

Mutations in the VapC dimer interface abolish conditional cooperativity

The $VapC^{Y72A}$ variant that was defective in dimerization yielded a possibility to test directly, *in vitro*, if indeed VapC dimerization is required for efficient binding of VapBC to *vapO* DNA. More importantly, however, we could also test if conditional cooperativity depends on VapC dimerization. We used purified VapB, VapC and $VapC^{Y72A}$ (Figure 5C). As expected, low concentrations of wild-type VapC increased binding of VapB to *vapO1* and higher concentrations destabilized the complex. A dramatically different pattern was seen with $VapC^{Y72A}$. First, a much higher concentration of $VapC^{Y72A}$ was required to yield efficient binding, consistent with the prediction that VapC dimers bridges two VapB dimers bound to operator DNA. However, strikingly, high concentrations of $VapC^{Y72A}$ did not destabilize the $VapBC^{Y72A}$ complex. On the contrary, increasing [$VapC^{Y72A}$] led to a strong increase in binding. VapC variants carrying other changes in the dimerization patches ($VapC^{Y72A}$, $VapC^{L43A}$, $VapC^{I44A}$ and $VapC^{A76S}$) behaved similarly although less dramatic (Supplementary Figure S4). The reduced capability of $VapC^{L43A}$ and $VapC^{A76S}$ to increase binding of VapB to *vapO1* (Supplementary Figure S4) is consistent with the increased transcription rates of *vapBC* loci carrying the corresponding alleles (Figure 5B). These observations show that not only is dimerization of VapC crucial for cooperative binding of $VapB_2$ to *vapO* but also for excess VapC to destabilize VapBC*O*.

DISCUSSION

We show here that *vapBC* of *S. enterica* is under complex transcriptional regulation by VapB and VapC: in the presence of an excess of VapB, VapC induced avid and cooperative binding of the VapBC complex to *vapO* operator DNA whereas an excess of VapC destabilized VapBC*O* (Figures 2–4). Band shifting with a *vapO* DNA fragment encoding both *vapO1* and *vapO2* yielded two different nucleoprotein complexes (Figure 2A) and mutations in *vapO1* or *vapO2* abolished VapBC binding at the mutated *vapO* operator but not at the other, intact operator (Figure 4B). Consistently, foot printing analysis revealed that the VapBC protected regions corresponding to *vapO1* and *vapO2* (Figures 2B and 3B). We conclude that the VapBC complex binds cooperatively to *vapO1* and *vapO2* in the presence of excess VapB.

In contrast, an excess of VapC destabilized VapBC binding to both *vapO1* and *vapO2* (Figure 3A and B) and, consistently, overexpression of a non-toxic variant of VapC in living cells stimulated transcription (Figure 3C and D). Transcription of *vapBC* is thus regulated by conditional cooperativity. Remarkably, a DNA fragment carrying only one operator (*vapO1*) responded similarly, showing that the two operator sites function

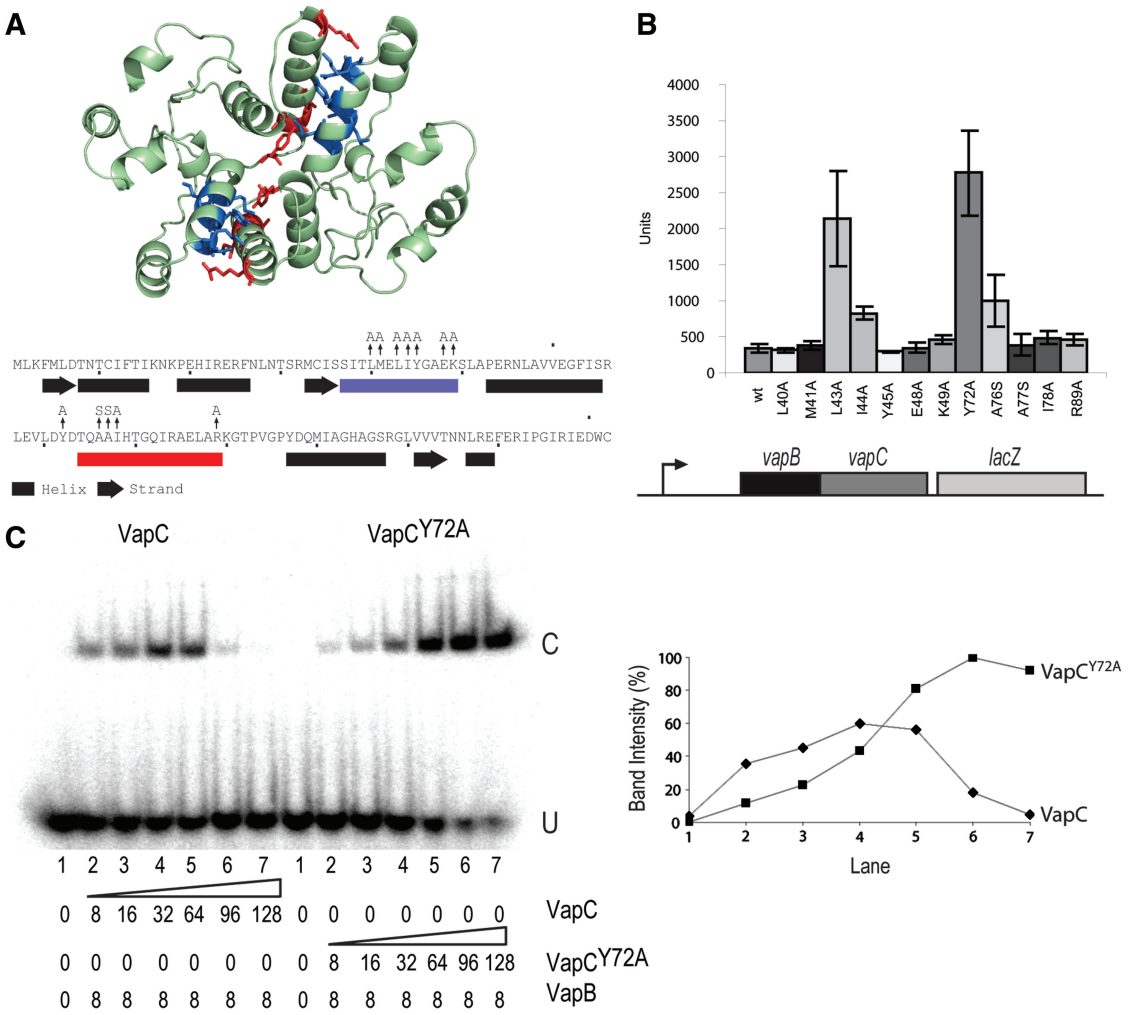

Figure 5. VapC dimerization is required for conditional cooperativity. (**A**) Predicted tertiary structure of a VapC dimer showing positions of amino acid changes in the dimer interface. The predicted secondary structure of VapC is shown below the primary sequence. Amino acid patches involved in dimerization are shown in blue and red, and amino acid substitutions in these patches are indicated by vertical arrows. (**B**) LacZ activities of *vapBC::lacZ* transcriptional fusions carrying mutations in *vapC*. The genetic set-up of the transcriptional *vapBC::lacZ* fusion used is shown schematically below the diagram. A broken arrow pointing rightward indicates the *vapBC* promoter. TB28 (MG1655Δ*lacZIYA*) containing pKW254BC (*vapBC*::*lacZYA*) or its isogenic *vapC* substitution mutant derivatives (see Supplementary Table S1) were grown exponentially in LB medium at 37°C and specific LacZ activities were determined. (**C**) Gel shifts of *vapO1* DNA with VapB and VapC (left panel) or VapC^{Y72A} (right panel). The proteins were mixed with radio labelled *vapO1* DNA in given concentrations (nM) (lanes 1–7). U and C indicate positions of unbound and bond complexes, respectively. Right: Quantification of C band intensities (%) seen in (C) as a function of lane number in the gel-shift shown at left.

independently and that one operator site is sufficient for conditional cooperativity (Figure 4B and D). The *vapO1* fragment bound a complex with a molecular weight consistent with the binding of an octamer of four VapB–VapC heterodimers $[(VapBC)_2]_2$, a stoichiometry similar to that of a VapBC (FitAB) complex from *N. gonorrhoea* bound to DNA (29). In this complex, VapB dimers bound to each operator half-site are bridged by VapC dimers (Supplementary Figure S1D). A similar stoichiometry has also recently been shown for the DNA-bound VapBC complex of *Rickettsia felis* (35). In addition, Brodersen and co-workers showed that VapBC from *S. flexneri* pMYSH6000 forms a complex of similar stoichiometry (Supplementary Figure S1C) (33). These scientists also showed that VapBC binds to two operator sites forming complexes of similar sizes. Figure 6 presents a model explaining how the VapB/VapC ratio controls the formation of the complex of VapBC with a single operator site by conditional cooperativity. First, the strong cooperative binding of VapBC to an operator site is explained by the two VapC dimers that bridge the two VapB dimers each recognizing the operator half-sites. Secondly, the bridging by the VapC dimers in the complex makes VapC dimerization the controlling element in the cooperative binding of the complex: with an excess of VapB, a stable $[(VapBC)_2]_2$ complex binds cooperatively to an operator site. In contrast, with an excess of VapC, VapC destabilizes VapBC bound to an operator site by invading the complex and breaking the VapC dimer.

We challenged the model experimentally by alanine/serine scanning of the patches in VapC responsible for

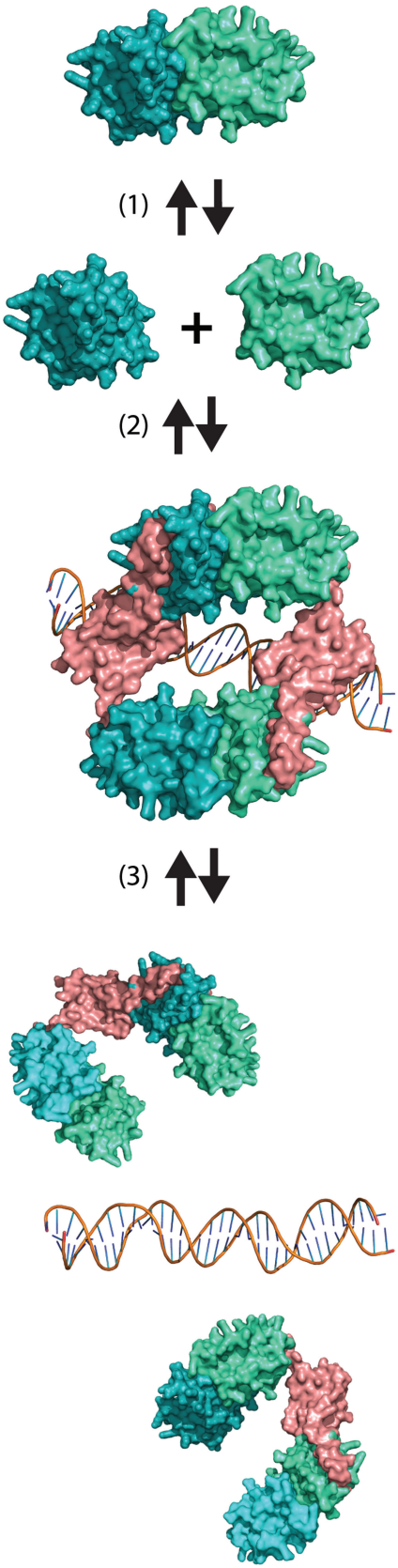

Figure 6. Molecular model explaining destabilization of the VapBC complex bound to a single operator site by VapC. (i) VapC dimer exist in an equilibrium with two VapC monomers. (ii) When VapC is in excess of VapB, VapC monomers 'invade' the VapBC*O* complex. (iii) Invasion abrogates cooperativity of VapBC*O* complex binding and decreases the affinity of VapBC for DNA. The structures shown were modelled, using the known structure of the $[(FitAB)_2]_2$ •DNA complex (29).

dimerization (Figure 5A). Four of the 12 single amino acid changes that were tested significantly reduced transcriptional repression by VapBC (Figure 5B), consistent with the model. In particular, the Y72A change in VapC completely abolished repression. The corresponding amino acid in VapC of *N. gonorrhoea* (P78) has previously been shown to be important for VapC dimerization (29) (Supplementary Figure S1B). We confirmed that this was also the case for VapC; $VapC^{Y72A}$ only showed weak dimerization *in vitro* (Supplementary Figure S3). We conclude that VapC forms dimers, both in solution and in the VapBC*O* repression complex.

We then analysed the VapC variants that exhibited a reduced ability to repress transcription *in vivo* and in *in vitro* (Figure 5B and C). The changes were dramatic: The $vapBC^{Y72A}$ operon was strongly de-repressed and, consistently, the Y72A substitution reduced VapBC complex formation with *vapO1*. Most importantly, however, the binding-response of $VapBC^{Y72A}$ was non-cooperative and an excess $VapC^{Y72A}$ did not destabilize the $VapBC^{Y72A}O$ complex (Figure 5C). A similar abrogation of VapBC*O* complex destabilization was seen with the other mutants that exhibited reduced transcriptional repression *in vivo* (Supplementary Figure S4). Thus, VapC dimerization is key, not only to repression but also to derepression of *vapBC* transcription, that is, for conditional cooperativity. These results support a model in which both formation and destabilization of VapBC*O* is controlled by VapC dimerization. In particular, destabilization is caused by a VapC monomer switching partner by pairing with a VapC monomer within the VapBC*O* complex and thereby breaking the bridging dimer required for strong and cooperative binding of VapBC to *vapO* (Figure 6). In all cases, the amino acid changes in VapC that conferred reduced repression *in vivo* (Figure 5B) also abolished VapBC*O* destabilization *in vitro* (Supplementary Figure S4). These results lend further support to the model.

Conditional cooperativity has been described to control TA operon transcription in three evolutionary independent gene families, *ccd* of F, *relBE* of *E. coli* and *phd-doc* of P1 and is understood at the mechanistic level for all three families (2,3,24,36). RelB antitoxin dimers bind *relO* operator half-sites via their Ribbon–Ribbon–Helix motifs (37). We previously proposed a model in which RelE has two binding sites for RelB, a high-affinity and a low-affinity site and that one RelE monomer bridges two RelBs belonging to two different dimers bound to operator half-sites (23). In this model, excess RelE destabilized RelBE*O* by invasion of a second RelE molecule into the complex by breaking the interaction between the low-affinity-site between RelE and RelB. Thus, a high-affinity interaction replaced a low-affinity interaction and was consistent with a very high efficiency of complex destabilization—that is—RelBE*O* was

destabilized already when the RelE/RelB ratio exceeded 1 and at a ratio of approximately 2, the entire RelBE*O* complex had disintegrated. In contrast, complete destabilization of VapBC*O* occurred at a VapC/VapB ratio >16, that is, destabilization of the VapBC*O* complex occurred gradually and required a much higher relative level of VapC. This considerably lower sensitivity of conditional cooperativity in *vapBC* regulation can be explained by the model in Figure 6: VapC is a dimer in solution that will be in equilibrium with two monomers. The monomers will also be in equilibrium with the dimers in VapBC*O* but competition is in this case between molecules with identical affinities, assuming that the dimer interface in a VapC dimer is the same as that of a VapC dimer in VapBC*O*. Therefore, in VapBC*O*, the VapC dimer equilibrium will be pushed towards complex destabilization and dimer breaking by high VapC concentrations. The observations made in this study support that under conditions when VapC is in excess of VapB, VapC can directly promote transcription of *vapBC* and thereby stimulate VapB production to help regenerate a balanced VapB/VapC ratio. Whether this mechanism is active during physiological conditions still needs to be tested.

Conditional cooperativity in the case of the *phd-doc* operon control is understood at a profound mechanistic level that lends support to the above-proposed model of how RelE controls *relBE* transcription (24). Using a direct structural approach, Remy Loris and colleagues showed that Doc toxin has both a low-affinity and high-affinity binding site for the C-terminus of the Phd antitoxin, similar to what we postulated for the RelBE interaction as described earlier. Structural analysis of Phd in the presence and absence of Doc showed that binding of Doc to Phd changed a partly disordered DNA binding domain to an ordered one and thereby increased the affinity of Phd for is operator. Due to the second, low affinity binding-site in Doc, one Doc molecule is able to bridge two Phd dimers bound to DNA and thereby confer cooperativity. Thus, Doc has two separate effects on DNA binding of Phd to its operator, both of which increase binding. At a high Doc/Phd ratio, further Doc molecules invade and destabilise the Doc–Phd–operator complex. These considerations raise the possibility that the mechanisms by which Doc and RelE mediate conditional cooperativity may be mechanistically related even though the TA loci encoding these components evolved independently. It is also clear from the results presented here, that the molecular mechanisms of conditional cooperativity in the cases of *vapBC* on the one hand and *phd-doc*/*relBE* on the other are entirely different.

It has now become clear that conditional cooperativity is a property common to TA loci (all TA loci investigated so far are regulated by conditional cooperativity) and it is relevant to ask how conditional cooperativity relates to the biological function of TA loci. We showed recently that TA loci that encode RNases are required for persistence of *E. coli* (15). We proposed a model in which Lon, in a minor fraction of the cells, degrade the antitoxins and thereby induce toxin activity, dormancy and persistence (drug tolerance). The *vapBC* locus has all the properties required to function in persistence: it encodes a tRNase whose activity inhibits translation reversibly (25,32) and Lon degrades VapB antitoxin (Figure 1). It is not known how bacterial cells resuscitate from the dormancy that is characteristic of the persistent state (38). Persister cells have higher TA transcription-rates than the average cell population (39,40). This suggests that persisters have increased T/A ratios and therefore raises the possibility that conditional cooperativity is operative in persister cells. It is thus possible that conditional cooperativity secures a high, on-going transcription rate of TA loci in dormant cells and thereby allow *de novo* synthesis of antitoxin that quench the toxins. By inference, such quenching of the toxins must be required for the persisters to escape dormancy and resuscitate. A second possibility, not mutually exclusive with first, is that conditional cooperativity functions to rapidly turn off toxin activity and TA operon transcription. The latter possibility would also imply that conditional cooperativity help reduce fortuitous events of toxin activation due to random fluctuations (noise) in the antitoxin level.

VapC activity and transcription of *vapBC* are both regulated by Lon because the protease degrades VapB antitoxin (Figure 1). It is not yet known if degradation of VapB by Lon is controlled by cellular signals. It is tempting to speculate that VapB degradation is actively regulated by as yet unknown factors that control Lon activity because such active regulation would enable the cell to turn TA locus activity on and off according to internal or external stimuli. We are now pursuing this question.

SUPPLEMENTARY DATA

Supplementary Data are available at NAR Online: Supplementary Tables S1 and S2, Supplementary Figures S1–4, Supplementary Material and Methods and Supplementary References [25,29,32,33,41–44].

ACKNOWLEDGEMENTS

We thank Ditlev Brodersen for critical reading of the manuscript and the members of the Centre for Bacterial Cell Biology for stimulating discussions.

FUNDING

Funding for open access charge: Wellcome Trust.

Conflict of interest statement. None declared.

REFERENCES

1. Fozo,E.M., Hemm,M.R. and Storz,G. (2008) Small toxic proteins and the antisense RNAs that repress them. *Microbiol. Mol. Biol. Rev.*, **72**, 579–589.
2. Gerdes,K. and Wagner,E.G. (2007) RNA antitoxins. *Curr. Opin. Microbiol.*, **10**, 117–124.
3. Gerdes,K., Christensen,S.K. and Lobner-Olesen,A. (2005) Prokaryotic toxin-antitoxin stress response loci. *Nat. Rev. Microbiol.*, **3**, 371–382.

4. Fineran,P.C., Blower,T.R., Foulds,I.J., Humphreys,D.P., Lilley,K.S. and Salmond,G.P. (2009) The phage abortive infection system, ToxIN, functions as a protein-RNA toxin-antitoxin pair. *Proc. Natl Acad. Sci. USA*, **106**, 894–899.
5. Jørgensen,M.G., Pandey,D.P., Jaskolska,M. and Gerdes,K. (2009) HicA of Escherichia coli defines a novel family of translation-independent mRNA interferases in bacteria and archaea. *J. Bacteriol.*, **191**, 1191–1199.
6. Makarova,K.S., Wolf,Y.I. and Koonin,E.V. (2009) Comprehensive comparative-genomic analysis of type 2 toxin-antitoxin systems and related mobile stress response systems in prokaryotes. *Biol. Direct.*, **4**, 19.
7. Gerdes,K. (2000) Toxin-antitoxin modules may regulate synthesis of macromolecules during nutritional stress. *J. Bacteriol.*, **182**, 561–572.
8. Pandey,D.P. and Gerdes,K. (2005) Toxin - antitoxin loci are highly abundant in free-living but lost from host-associated prokaryotes. *Nucleic Acids Res.*, **33**, 966–976.
9. Shao,Y., Harrison,E.M., Bi,D., Tai,C., He,X., Ou,H.Y., Rajakumar,K. and Deng,Z. (2010) TADB: a web-based resource for Type 2 toxin-antitoxin loci in bacteria and archaea. *Nucleic Acids Res.*, **39**, D606–D611.
10. Ramage,H.R., Connolly,L.E. and Cox,J.S. (2009) Comprehensive functional analysis of *Mycobacterium tuberculosis* toxin-antitoxin systems: implications for pathogenesis, stress responses, and evolution. *PLoS Genet.*, **5**, e1000767.
11. Gerdes,K., Rasmussen,P.B. and Molin,S. (1986) Unique type of plasmid maintenance function: postsegregational killing of plasmid-free cells. *Proc. Natl Acad. Sci. USA*, **83**, 3116–3120.
12. Szekeres,S., Dauti,M., Wilde,C., Mazel,D. and Rowe-Magnus,D.A. (2007) Chromosomal toxin-antitoxin loci can diminish large-scale genome reductions in the absence of selection. *Mol. Microbiol.*, **63**, 1588–1605.
13. Christensen,S.K., Mikkelsen,M., Pedersen,K. and Gerdes,K. (2001) RelE, a global inhibitor of translation, is activated during nutritional stress. *Proc. Natl Acad. Sci. USA*, **98**, 14328–14333.
14. Tsilibaris,V., Maenhaut-Michel,G., Mine,N. and Van,M.L. (2007) What is the benefit to Escherichia coli of having multiple toxin-antitoxin systems in its genome? *J. Bacteriol.*, **189**, 6101–6108.
15. Maisonneuve,E., Shakespeare,L.J., Jorgensen,M.G. and Gerdes,K. (2011) Bacterial persistence by RNA endonucleases. *Proc. Natl Acad. Sci. USA*, **108**, 13206–13211.
16. Hallez,R., Geeraerts,D., Sterckx,Y., Mine,N., Loris,R. and Van,M.L. (2010) New toxins homologous to ParE belonging to three-component toxin-antitoxin systems in Escherichia coli O157:H7. *Mol. Microbiol.*, **76**, 719–732.
17. Nariya,H. and Inouye,M. (2008) MazF, an mRNA interferase, mediates programmed cell death during multicellular Myxococcus development. *Cell*, **132**, 55–66.
18. Christensen-Dalsgaard,M., Jorgensen,M.G. and Gerdes,K. (2010) Three new RelE-homologous mRNA interferases of Escherichia coli differentially induced by environmental stresses. *Mol. Microbiol.*, **75**, 333–348.
19. Christensen,S.K., Pedersen,K., Hansen,F.G. and Gerdes,K. (2003) Toxin-antitoxin loci as stress-response-elements: ChpAK/MazF and ChpBK cleave translated RNAs and are counteracted by tmRNA. *J. Mol. Biol.*, **332**, 809–819.
20. Gotfredsen,M. and Gerdes,K. (1998) The Escherichia coli relBE genes belong to a new toxin-antitoxin gene family. *Mol. Microbiol.*, **29**, 1065–1076.
21. Magnuson,R., Lehnherr,H., Mukhopadhyay,G. and Yarmolinsky,M.B. (1996) Autoregulation of the plasmid addiction operon of bacteriophage P1. *J. Biol. Chem.*, **271**, 18705–18710.
22. Magnuson,R. and Yarmolinsky,M.B. (1998) Corepression of the P1 addiction operon by Phd and Doc. *J. Bacteriol.*, **180**, 6342–6351.
23. Overgaard,M., Borch,J., Jorgensen,M.G. and Gerdes,K. (2008) Messenger RNA interferase RelE controls relBE transcription by conditional cooperativity. *Mol. Microbiol.*, **69**, 841–857.
24. Garcia-Pino,A., Balasubramanian,S., Wyns,L., Gazit,E., De,G.H., Magnuson,R.D., Charlier,D., van Nuland,N.A. and Loris,R. (2010) Allostery and intrinsic disorder mediate transcription regulation by conditional cooperativity. *Cell*, **142**, 101–111.
25. Winther,K.S. and Gerdes,K. (2011) Enteric virulence associated protein VapC inhibits translation by cleavage of initiator tRNA. *Proc. Natl Acad. Sci. USA*, **108**, 7403–7407.
26. Wilbur,J.S., Chivers,P.T., Mattison,K., Potter,L., Brennan,R.G. and So,M. (2005) Neisseria gonorrhoeae FitA interacts with FitB to bind DNA through its ribbon-helix-helix motif. *Biochemistry*, **44**, 12515–12524.
27. Bodogai,M., Ferenczi,S., Bashtovyy,D., Miclea,P., Papp,P. and Dusha,I. (2006) The ntrPR operon of Sinorhizobium meliloti is organized and functions as a toxin-antitoxin module. *Mol. Plant Microbe Interact.*, **19**, 811–822.
28. Robson,J., McKenzie,J.L., Cursons,R., Cook,G.M. and Arcus,V.L. (2009) The vapBC operon from Mycobacterium smegmatis is an autoregulated toxin-antitoxin module that controls growth via inhibition of translation. *J. Mol. Biol.*, **390**, 353–367.
29. Mattison,K., Wilbur,J.S., So,M. and Brennan,R.G. (2006) Structure of FitAB from Neisseria gonorrhoeae bound to DNA reveals a tetramer of toxin-antitoxin heterodimers containing pin domains and ribbon-helix-helix motifs. *J. Biol. Chem.*, **281**, 37942–37951.
30. Sambrook,J., Fritsch,E.F. and Maniatis,T. (1989) *Molecular Cloning: A Laboratory Manual*, 2nd edn. Laboratory Press, Cold Spring Harbor, New York.
31. Hunter,S., Apweiler,R., Attwood,T.K., Bairoch,A., Bateman,A., Binns,D., Bork,P., Das,U., Daugherty,L., Duquenne,L. *et al.* (2009) InterPro: the integrative protein signature database. *Nucleic Acids Res.*, **37**, D211–D215.
32. Winther,K.S. and Gerdes,K. (2009) Ectopic production of VapCs from Enterobacteria inhibits translation and trans-activates YoeB mRNA interferase. *Mol. Microbiol.*, **72**, 918–930.
33. Dienemann,C., Boggild,A., Winther,K.S., Gerdes,K. and Brodersen,D.E. (2011) Crystal Structure of the VapBC toxin-antitoxin complex from Shigella flexneri reveals a hetero-octameric DNA-binding assembly. *J. Mol. Biol*, **414**, 713–722.
34. Kelley,L.A. and Sternberg,M.J. (2009) Protein structure prediction on the Web: a case study using the Phyre server. *Nat. Protoc.*, **4**, 363–371.
35. Mate,M.J., Vincentelli,R., Foos,N., Raoult,D., Cambillau,C. and Ortiz-Lombardia,M. (2012) Crystal structure of the DNA-bound VapBC2 antitoxin/toxin pair from Rickettsia felis. *Nucleic Acids Res.*, **40**, 3245–3258.
36. De,Jonge,N., Garcia-Pino,A., Buts,L., Haesaerts,S., Charlier,D., Zangger,K., Wyns,L., De,G.H. and Loris,R. (2009) Rejuvenation of CcdB-poisoned gyrase by an intrinsically disordered protein domain. *Mol. Cell*, **35**, 154–163.
37. Overgaard,M., Borch,J. and Gerdes,K. (2009) RelB and RelE of Escherichia coli form a tight complex that represses transcription via the ribbon-helix-helix motif in RelB. *J. Mol. Biol.*, **394**, 183–196.
38. Lewis,K. (2010) Persister cells. *Annu. Rev. Microbiol.*, **64**, 357–372.
39. Keren,I., Shah,D., Spoering,A., Kaldalu,N. and Lewis,K. (2004) Specialized persister cells and the mechanism of multidrug tolerance in Escherichia coli. *J. Bacteriol.*, **186**, 8172–8180.
40. Shah,D., Zhang,Z.G., Khodursky,A., Kaldalu,N., Kurg,K. and Lewis,K. (2006) Persisters: a distinct physiological state of E-coli. *BMC Microbiol.*, **6**, 53.
41. Miller,J.H. (1972) *Experiments in Molecular Genetics*. Laboratory Press, Cold Spring Harbor, New York.
42. Livak,K.J. and Schmittgen,T.D. (2001) Analysis of relative gene expression data using real-time quantitative PCR and the 2(-Delta Delta C(T)) method. *Methods*, **25**, 402–408.
43. Orchard,K. and May,G.E. (1993) An EMSA-based method for determining the molecular weight of a protein–DNA complex. *Nucleic Acids Res.*, **21**, 3335–3336.
44. Guzman,L.M., Belin,D., Carson,M.J. and Beckwith,J. (1995) Tight regulation, modulation, and high-level expression by vectors containing the arabinose PBAD promoter. *J. Bacteriol.*, **177**, 4121–4130.